

Medium- and Sensitizer-Dependent Radical Cation Reactions: Deprotonation in Fluid Solution and Solid Matrices†

Heinz D. Roth,^{a,*} Hengxin Weng,^a Dahui Zhou^a and Prasad S. Lakkaraju^b

^aRutgers University, Department of Chemistry, New Brunswick, NJ 08855-0939, USA and ^bGeorgian Court College, Department of Chemistry, Lakewood, NJ 08701, USA

Roth, H. D., Weng, H., Zhou, D. and Lakkaraju, P. S., 1997. Medium- and Sensitizer-Dependent Radical Cation Reactions: Deprotonation in Fluid Solution and Solid Matrices. – Acta Chem. Scand. 51: 626–635. © Acta Chemica Scandinavica 1997.

Radical cations generated by photo-induced electron transfer in solution or by chemical oxidation in the channels of a redox-active zeolite (NaZSM-5) may be deprotonated, giving rise to neutral radicals. In solution, the geminate radical anion or an added nucleophile (methanol) may serve as the proton acceptor. Deprotonations in solution are not efficient; the corresponding products may be suppressed by several competing intra- or bi-molecular reactions. Although methanol serves as the base deprotonating at least one radical cation, it often is more efficient as a nucleophile, thereby depressing deprotonation. Deprotonations in the zeolite are more effective, presumably, because competing reactions with outside reagents are precluded. Occasionally, NaZSM-5 zeolites promote complex reaction sequences, such as the conversion of *p*-propylanisole to the radical cation of anethole or the deprotonation-ring opening of 1,2-diphenylcyclopropane radical cation to *exo,exo*-diphenylallyl radical.

The structures of organic radical cations have been the focus of much interest for the past two decades.^{1–4} A rich variety of substrates have been investigated by an array of physical and chemical techniques for the purpose of delineating changes in molecular geometry upon one-electron oxidation, assessing the spin density distribution in the resulting radical cations, and elucidating the parameters affecting the structures of these intermediates.^{4–7} In particular, the interactions between adjacent functions, conjugated or non-conjugated, pairs of olefinic π -systems or strained rings, or of strained ring moieties with olefinic fragments in organic radical cations has attracted considerable interest.^{5–7}

Similarly, radical cation reactions also have attracted much attention.^{8–16} As intermediates with both an unpaired spin and a positive charge, radical cations can undergo a variety of reactions characteristic for either free radicals or carbocations. Among bimolecular reactions, the additions of radical cations to alkenes⁸ and their nucleophilic capture by alcohols,^{9–11} which lead to C–C and C–O bond formation, respectively, have been investigated in detail. Among unimolecular reactions, the geometric isomerization of appropriate radical cations

have been studied¹² as well as several molecular rearrangements,^{13,14} including sigmatropic shifts.^{15,16}

The course of radical cation reactions is delineated by the structure and stereochemistry of the products and the fate of chiral or isotopic labels. The efficiency of competing radical cation reactions can be based on the yields of appropriate products. These features are determined by various factors. In addition to the distribution of unpaired spin and positive charge, and bond lengths and angles, that is, the electronic and geometric structure of a radical cation, the method by which a radical cation is generated is one of the most important factors affecting its reactivity. The method of generation determines the reaction partner, influences the choice of the medium (solvent or matrix), and limits the inclusion of accessible reagents.

In fluid solution, organic radical cations can be generated by methods such as photo-induced electron transfer,¹⁷ anodic oxidation, or chemical oxidation. The radical cations formed by these methods may show different behavior as a consequence of the different environments in which they arise. Radical cations generated by photo-induced electron transfer are formed as part of a radical ion pair (RIP), either in contact with the radical anion (CRIP) or as a solvent-separated pair (SSRIP).¹⁸ The special nature of these pairs and the

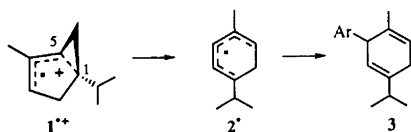
† Lecture held at the 14th International Conference on Radical Ions, Uppsala, Sweden, July 1–5, 1996.

* To whom correspondence should be addressed.

presence (and nature) of a radical anion may influence the ensuing reactions in specific ways. Anodic oxidation generates radical cations in an oxidizing environment, close to the surface of the anode. This may lead to the oxidation of a reaction product. Chemical oxidation generates radical cations in close proximity to a reducing agent as well as additional oxidant. However, it is possible to choose a reagent with a one-electron redox potential sufficient for the desired oxidation and a two-electron redox potential insufficient for further oxidation of the radical cation. In the case of non-soluble oxidants, the reaction may occur on the surface of the oxidant and, occasionally, lead to the observation of unusual species.¹⁹ Solid matrices containing redox-active centers may generate radical cations on external or internal surfaces; radical cations sequestered in the internal channels of a zeolite have significantly increased lifetimes,^{20,21} because they are protected from outside reagents. In addition to the redox reactivity, the zeolite may also serve to deprotonate appropriate radical cations, as shown by the formation of iminoxyl radicals from oximes.^{22,23}

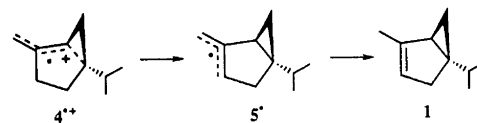
In this paper, we consider the generation and possible deprotonation of radical cations in two media, fluid solutions and the redox active sites of a zeolite, and compare the competing radical cation reactions in these media.

Deprotonation of radical cations in solution. In the course of the 1,4-dicyanobenzene (DCB) sensitized photochemistry of α -thujene (**1**), we observed an interesting product (**3**), formally derived by replacement of a hydrogen atom by an aryl group.¹⁶ The formation of this product was explained by deprotonation of the radical cation, $1^{+\cdot}$, and coupling of the resulting cyclohexadienyl radical, 2^{\cdot} , with the sensitizer radical anion, $DCB^{\cdot-}$. Loss of cyanide ion from the resulting 1,6-dicyanocyclohexadienyl anion completes the formation of **3**. Interestingly, this novel reaction occurred only in the presence of methanol, suggesting that methanol acts as the proton acceptor.

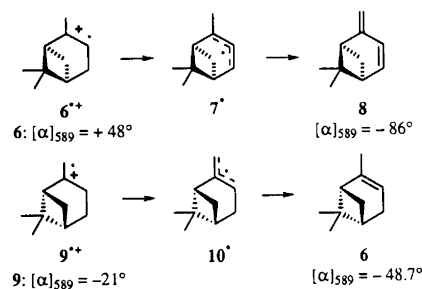


On the other hand, radical anions such as semiquinones are sufficiently strong bases to deprotonate radical cations. For example, the chloranil (Chl)-sensitized photoreaction of sabinene (**4**) resulted in the partial conversion into **1** (~20% after 4 min irradiation). This reaction is again explained via deprotonation, most likely by the semiquinone anion and within a geminate radical ion pair. Interestingly, with acetone- d_6 as the solvent, the α -thujene (**1**) formed has incorporated 40% of one deuterium into the allylic methyl group. Accordingly, the free radical, 5^{\cdot} , reacts by two pathways, deuterium abstraction from the solvent or hydrogen atom transfer from $\cdot Chl-H$. The protonation of quinone radical

anions has ample precedent²⁴⁻²⁷ as does the hydrogen atom transfer from $\cdot Chl-H$.²⁸

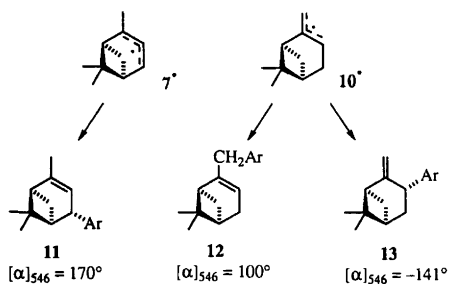


In a similar reaction, the photoreactions of α - (**6**) and β -pinene (**9**) with Chl as sensitizer in acetonitrile resulted in the formation of verbenene (**8**) and α -pinene (**6**), respectively; both reactions proceed with essentially quantitative retention of optical purity.²⁹ The conversion of $9^{+\cdot}$ into **6** is efficient and essentially irreversible; no β -pinene is observed in the reaction of **6**. These findings can be rationalized via the deprotonation of α - and β -pinene radical cations, $6^{+\cdot}$ and $9^{+\cdot}$, respectively, by chloranil semiquinone, $Chl^{\cdot-}$. The allylic free radical, 10^{\cdot} , derived from β -pinene serves as a regioselective H-atom acceptor towards $Chl-H^{\cdot}$ whereas the free radical, 7^{\cdot} , formed from α -pinene reacts, in part, by H-atom transfer (disproportionation) to the semiquinone radical ($\cdot Chl-H$). The regioselective protonation of 10^{\cdot} is a key step in the conversion of **9** into **6** via $9^{+\cdot}$ and 10^{\cdot} . The selectivity reflects the greater thermodynamic stability of the endocyclic relative to the exocyclic olefin.



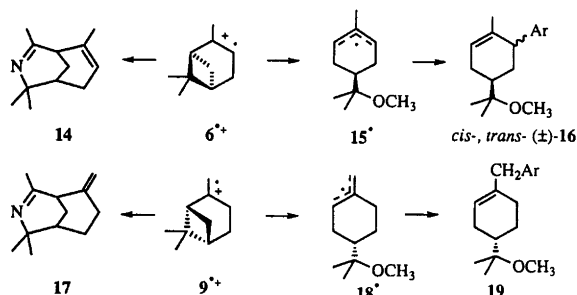
The photoreactions of **6** and **9** with DCB as sensitizer produce two isomeric hydrocarbons and three aryl-substituted vinylcyclobutane compounds, **11**–**13**. Both product types are rationalized via the radical cations, $6^{+\cdot}$ and $9^{+\cdot}$. Although DCB radical anion ($DCB^{\cdot-}$) is a weaker base than the semiquinone anions, two allylic free radicals, 7^{\cdot} and 10^{\cdot} , are formed by proton transfer from either radical cation to $DCB^{\cdot-}$, in competition with ring opening (*vide infra*). The free radicals couple with the protonated sensitizer radical anion, $DCB-H^{\cdot-}$; the resulting 2,5-dicyanocyclohexa-1,4-diene derivatives generate products **11**–**13** by loss of hydrogen cyanide. The net reaction amounts to substitution of an allylic hydrogen atom by a cyanophenyl group via an electron transfer induced 'addition-elimination' pathway. This mechanism is a variation of that invoked for the formation of **3**.

All three products show high optical rotations; **11** has been isolated whereas **12** and **13** proved difficult to separate. Nevertheless, we could assign approximate specific rotations to them. We were able to obtain samples of different compositions (and different rotations). The NMR spectra of **12** and **13** are sufficiently different,

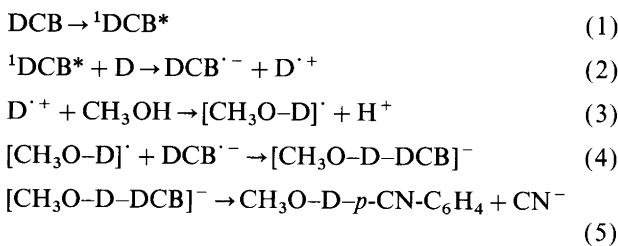


allowing us to determine the composition by NMR integration as well as the specific rotations.

The electron transfer photochemistry of DCB with **6** and **9** in acetonitrile-methanol has been studied before.^{30,31} Under these conditions, the radical cations, **6**^{•+} and **9**^{•+}, react by nucleophilic capture with methanol and, to a lesser extent, with acetonitrile. The reaction with methanol generates methoxy-substituted free radicals, **15**[•] and **18**[•], whereas the reaction with acetonitrile produces bicyclic acetonitrile adducts, **14** and **17**. The free radicals, **15**[•] and **18**[•], couple with the sensitizer anion followed by loss of cyanide ion; this reaction gives rise to so-called NOCAS products (for nucleophile-olefin combination aromatic substitution), e.g., *cis*- and *trans*-**16** and **19** (and isomers), respectively.



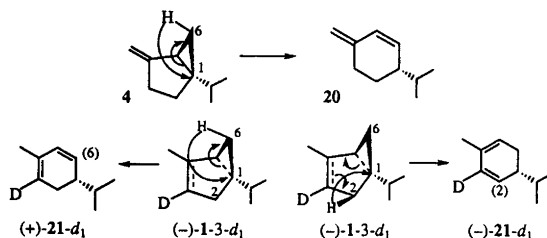
Three-component coupling products of this type are formed frequently in the DCB sensitized electron transfer reactions with cyclopropane derivatives or olefins in the presence of methanol.^{32,33} These products are rationalized via a general reaction sequence (Scheme 1) formulated for the reaction of a donor, D, with DCB. The final steps in this mechanism [eqns. (4)–(5)], delineating a two-step 'aromatic substitution', are essentially identical with the previously discussed reactions leading to the formation of product **3** from **1**^{•+} and **11–13** from **6**^{•+}, respectively.



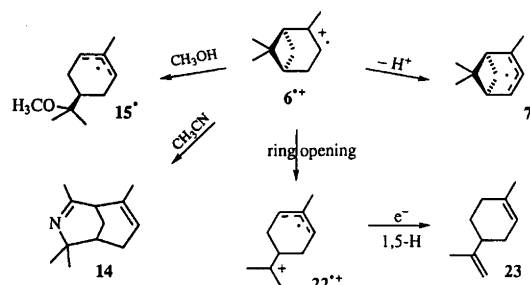
Scheme 1.

In the photoreaction of DCB with **6** and **9**, methanol does not serve as a base, deprotonating **6**^{•+} and **9**^{•+}; in fact, its nucleophilic addition to the radical cations suppresses the deprotonation by $\text{DCB}^{\cdot-}$. This reaction generated only 1–2% of products **11–13**, vs. 7–8% each in the absence of methanol. The high optical rotation of products **11–13** and **8** and **6**, formed by the chloranil-sensitized reaction of **6** and **9**, respectively, requires 'ring-closed' vinylicyclobutane radical cations, whereas 'ring-opened' species have been invoked in the formation of NOCAS products with DCB.^{30,31} *Ab-initio* calculations support the existence of both ring-closed and ring-opened radical cations.^{31,34,35}

In fact, the deprotonation is suppressed not only by nucleophilic capture, but by several other competing reactions as well. Assorted radical cations rearrange by sigmatropic shift of a hydrogen atom. Thus, a [1,3] sigmatropic shift of sabinene radical cation, **4**^{•+}, generates β -phellandrene radical cation, **20**^{•+}, a ring-opened species with extended conjugation.¹⁶ Similarly, **1** is converted into α -phellandrene (**21**); in this system, the [1,3] shift competes with a homo-[1,5] sigmatropic shift; the dual reaction was established by a deuterium label at C-3. Rearrangements of several other radical cations may involve [1,3] sigmatropic shifts; on the other hand, the homo-[1,5] shift appears to be unique.¹⁶



Finally, we mention the ring opening of **6**^{•+}, generating limonene, **23** (apparently via the ring-opened pinene radical cation, **22**^{•+}), as a further unimolecular reaction competing with deprotonation.^{29–31} This reaction can be formulated by back electron transfer to the rearranged radical cation, **22**^{•+}, and a 1,5-H shift in the resulting biradical. This reaction has precedent in the electron transfer induced cyclizations of geraniol.³⁶



In summary, we have observed the deprotonation of several radical cations of unsaturated and strained ring hydrocarbons, usually from an allylic carbon.

Appropriate proton acceptors include semiquinone radical anions, dicyanobenzene radical anion or, in at least one case, methanol. Various intra- and inter-molecular reactions compete with deprotonation, including nucleophilic capture by methanol or acetonitrile, back electron transfer, sigmatropic shifts, or rearrangements (ring opening). Because several of the competing reactions are more efficient, the deprotonation of radical cations in solution frequently are inefficient.

Generation and deprotonation of radical cations in zeolites.

The second environment in which we have studied radical cation formation and, in some cases, deprotonations are the channels of a pentasil zeolite, Na-ZSM-5. During the past thirty years the structures and catalytic properties of zeolites have been extensively investigated and many chemical reactions on the surface and in the micropores have been studied.³⁷⁻⁴⁰ Recently, a method for the generation of π -type radical cations within the nearly cylindrical channels (ID ~ 5.5 Å) of pentasil zeolite at ambient temperatures has been reported; this method appears to be general in scope and simple in practice.^{20,21} The detailed nature of the redox-active site in the zeolite is subject to speculation and debate;⁴¹⁻⁴⁵ however, an approximate redox potential ($E_{\text{ox}} \sim +1.65$ V vs. SCE) has been determined empirically.^{20,21} The resulting radical cations appear to be held rigidly in the channels of the zeolite; this may account for their increased stability; the radical cations have very long lifetimes and, hence, can be studied by conventional spectroscopic techniques.^{20,21}

We have applied this method to a range of substrates, including hydrocarbons, phenol ethers and dialkylanilines, and have observed various interesting radical cations which are stable at room temperature. We also extended the scope of this method to the generation of σ -type neutral radicals (iminoxyls) from oximes.^{22,23} In the formation of the resulting free radicals the zeolite played the dual role of one-electron oxidant and proton acceptor. While π -type radicals have been previously generated in zeolites, our experiments were the first to succeed in the generation of σ -type radicals, species in which the spin is localized in the N–O function of the molecule and is not delocalized into the C=N bond. Similar to the nature of the redox-active centers in the pentasil zeolite, the site involved in the deprotonation and the detailed mechanism of the oxidation–deprotonation is also subject to speculation.

Because of the formal relationship between the deprotonations in the zeolite and those observed in solution, we considered the oxidation and, as appropriate, deprotonation of simple substrates in the channels of a pentasil zeolite, Na-ZSM-5. We illustrate the types of substrate that may be oxidized, and subsequent reactions of the resulting radical cations, with EPR spectra observed upon incorporating several anisole derivatives and *p*-methylphenol into the zeolite.

Incorporation of these substrates into the channels of

Na-ZSM-5 zeolite causes light colorations in the sample. After being washed and dried, the zeolite samples loaded in this fashion show strong and persistent EPR spectra characteristic of organic free radicals with linewidths ≤ 2 G. The radicals appear to be sequestered in the channels of the zeolite, since radicals formed on the external surface of the zeolite would either decay or be removed by washing. Indeed, the light coloration observed upon mixing the reagents is likely due to free radicals or radical ions on the external surface of the zeolite. Some of the coloration is removed by washing, suggesting that the corresponding radicals are removed from the external surface of the zeolite.

The generation and observation of paramagnetic species in a solid matrix such as Na-ZSM-5 zeolite raises several questions, including the identity of the species so generated, their mobility (which manifests itself in the isotropic or anisotropic appearance of the spectrum), the location of the species in the host matrix and its interaction with any specific site, and whether the particular environment may change the intrinsic properties of the paramagnetic species. It is generally recognized that the access of reagents to the reactive species is blocked; this is born out by the significantly increased lifetimes of species generated in the zeolite. Typical lifetimes of radicals or radical ions generated in Na-ZSM-5 zeolite are 2–3 days. By comparison, many radical cations could only be studied in flow systems,⁴⁶ although some relatively inert solvent systems have been developed.^{47,48}

The addition of two phenol ethers, *p*-methylanisole (**24**) and *p*-methylethoxybenzene (**25**) to a suspension of the zeolite in dry 2,2,4-trimethylpentane gave rise to faintly colored samples. After washing and evaporation of the solvent the dried zeolite showed well resolved EPR spectra, featuring a quartet of quartets ($A = 15.0, 3.9$ G; $g = 2.0040$) and a quartet of triplets ($A_{3\text{H}} = 15.0$ G, $A_{2\text{H}} = 4.7$ G; $g = 2.0042$), respectively (Fig. 1). Since both methyl groups of **24** are coupled, the spectrum should be that of the radical cation, **24**^{•+}. This assignment is confirmed by the good agreement with the known spectrum of **24**^{•+} ($A_{\text{CH}_3} = 15.25$ G, $A_{\text{OCH}_3} = 4.3$ G; $g = 2.0032$), obtained by Ce^{IV} oxidation and recorded in a flow system.⁴⁶ The (minor) discrepancies are tentatively ascribed to matrix effects. The EPR spectrum observed upon incorporation of *p*-methylethoxybenzene into the zeolite is assigned to the corresponding radical cation, **25**^{•+}; the quartet splitting ($A_{\text{CH}_3} = 15.0$ G) is similar to that of **24**^{•+} and the lesser splitting ($A_{\text{CH}_2} = 4.7$ G) is in good agreement with the analogous splitting of the ethoxybenzene ($A_{\text{CH}_2} = 5.0$ G)⁴⁶ or the 2,6-di-*tert*-butyl-4-methylanisole radical cation ($A_4 = 13.3$ G; $A_1 = 3.6$ G).⁴⁹ These results support significant spin density on the *p*-carbons of the two radical cations.

An anisole derivative bearing an unsaturated side chain, *trans*-anethole (**26**), is oxidized with particular ease, giving rise to a pale blue sample. The EPR spectrum indicates the presence of an organic radical or radical cation ($g = 2.0032 \pm 0.0002$) with four strongly coupled

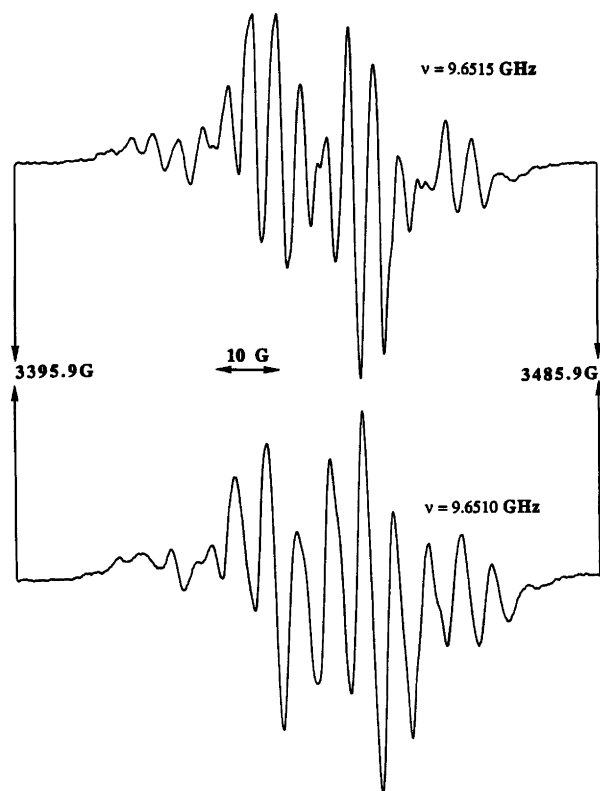


Fig. 1. X-Band EPR spectra of two radical cations sequestered in pentasil zeolite (Na ZSM-5). The spectrum of *p*-methylanisole radical cation ($22'^+$; $g=2.0040$) shows a quartet of quartets, with $A=15.0$ and 3.9 G, respectively (top); the spectrum of *p*-methylethoxybenzene radical cation ($23'^+$; $g=2.0042$), (bottom), shows a quartet of triplets with $A=15.0$ G (3 H) and $A=4.7$ G (2 H), respectively.

nuclei ($A \sim 11$ G; Fig. 2). The spectrum also documents the presence of at least two nuclei with smaller hfc. The central portion of the EPR spectrum is well resolved showing hfc's as small as 2 G. The linewidth increases upfield or downfield from the center, indicating that the

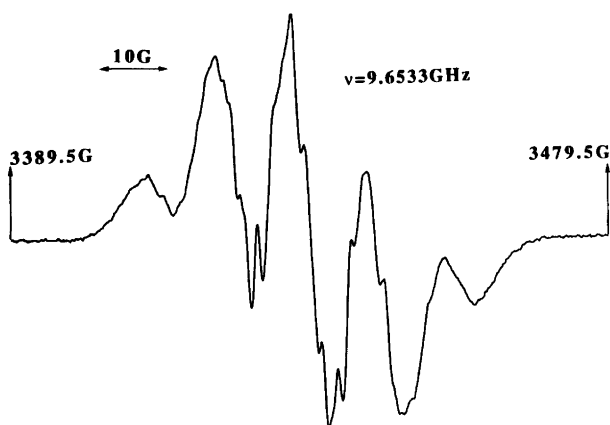
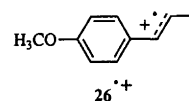


Fig. 2. X-Band EPR spectrum of anethole radical cation ($26'^+$), sequestered in pentasil zeolite (Na ZSM-5). The four strongly coupled ^1H nuclei in the radical cation ($A \sim 11$ G) are assigned as the olefinic β -proton and those of the allylic methyl group.

hyperfine and g factor anisotropies are not completely averaged. This finding suggests that the motion of the radical ion in the cavities of the zeolite is restricted.⁵⁰



The radical cation, $26'^+$, has been generated in solution by photo-induced electron transfer to triplet quinones.^{51–53} A CIDNP study found strong emission for the allylic methyl signal and strongly enhanced absorption for the olefinic β -signal, demonstrating a large positive hyperfine coupling (hfc) for the allylic nuclei and a sizeable negative hfc for the β -proton.⁵¹ Later CIDNP studies established that anethole cation–semiquinone anion pairs undergo back electron transfer from the triplet manifold, giving rise to Paterno–Büchi type oxetane products via triplet 1,4-biradicals.⁵² AM1 calculations showed significant hyperfine coupling constants for the allylic methyl group ($+4.9$ G), as well as the β - (-5.5 G) and α -protons ($+2.3$ G).⁵² In agreement with the CIDNP results, we identify the four strongly coupled nuclei as those of the allylic methyl group and the olefinic β -proton. Interestingly, the coupling constants measured in Na-ZSM-5 are twice as large⁵⁰ as the calculated ones.⁵² Both EPR and CIDNP data agree that the spin density of the anethole radical cation is located mainly in the olefinic side chain, regardless of the medium in which it is observed, zeolite or solution. Interestingly, the electronic spectrum of $26'^+$ has been recorded following pulse radiolysis.⁵⁴ Under these conditions the transient spectrum decays within microseconds, in marked contrast with the lifetime of several days in the zeolite.

For the substrates discussed so far, the zeolite functions only as a one-electron redox agent, generating radical cations, viz., $24'^+ - 26'^+$. However, for substrates containing more acidic ^1H nuclei, the oxidation may be followed by deprotonation. In special cases, even more complex reaction sequences may be initiated. The deprotonation of O and N acids appear to be particularly efficient; for example, oximes, phenols, and anilines are readily converted into iminoxyls,^{22,23} phenoxyls, and aniliny radicals. However, appropriate hydrocarbons may also be deprotonated.

The EPR spectrum observed upon inclusion of 1-phenylethane-1,2-dione 2-oxime (**27**) in Na-ZSM-5 shows features characteristic of an axially symmetric powder pattern with two overlapping 1:1:1 triplets.²³ The signals in the high field region revealed clearly resolved doublets, with $A=2.9$ and 8.9 G. The EPR spectrum supports a benzoyliminoxyl radical ($28'$) whose principal axes of ^{14}N and ^1H dipolar hyperfine couplings, $A_{\text{N},\parallel}$ and $A_{\text{H},\parallel}$, respectively, are nearly perpendicular to each other (Fig. 3). This assignment identified the iminoxyl as the *Z*-isomer.²³

Incorporation of simple phenols, e.g., *p*-methylphenol (**29**), into the channels of Na ZSM-5 zeolite leads to the

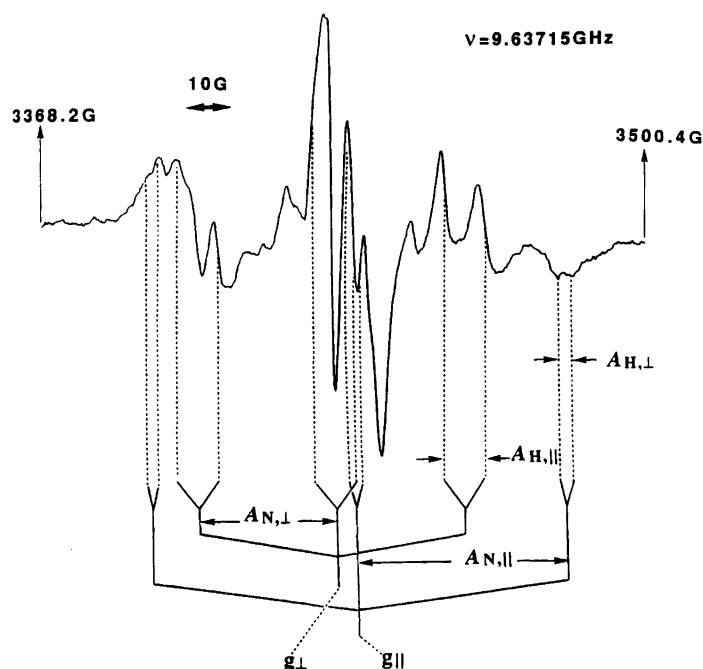
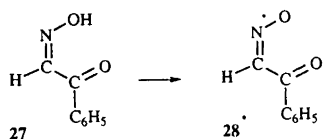


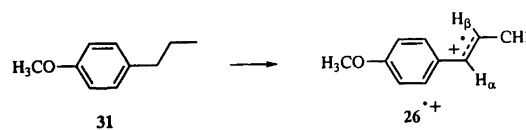
Fig. 3. X-Band EPR spectrum of benzoyliminoxyl radical (**28**) sequestered in pentasil zeolite (Na ZSM-5). The features assigned to the parallel and perpendicular components, $g_{\parallel} = 2.0030$, $A_{N,\parallel} = 44.1$ G, $A_{H,\parallel} = 8.8$ G, and $g_{\perp} = 2.0068$, $A_{N,\perp} = 29.1$ G, $A_{H,\perp} = 2.9$ G, respectively, are identified in the spectrum.²³



generation of phenoxyl radicals, e.g., *p*-methylphenoxyl (**30**; $g = 2.0042 \pm 0.0001$; $A = 14.6$ G, 3 H; linewidth = 2.1 G). The spectrum is complicated by powder-like features at the low and high field end and, presumably, throughout the spectrum. The identity of the resulting species is tentatively assigned based on the well resolved 1:3:3:1 quartet and by comparison with the known spectra of **30** ($A_{\beta} = 11.95$ G, 3 H; $A_{2,6} = 6.0$ G, 2 H)^{55,56} and of some sterically hindered phenoxyls.^{57,58} Typical phenoxyl radicals have significant spin density on the oxygen center as well as on the *o*- and *p*-carbons of the aromatic ring. The species sequestered in the zeolite shows the expected strong hyperfine coupling for the three methyl protons; however, there is no evidence for any significant coupling of the *o*-protons. In fact, the EPR spectrum obtained from **29-*d*₄** shows a very similar spectrum ($A_{\text{CH}_3} = 14.4$ G; linewidth = 1.3 G). These results may indicate a distortion of the conventional phenoxyl radical, **30**, by a specific interaction with the zeolite matrix. The observed spectra do not offer any evidence for the location of the species in the matrix or the detailed mechanism of the oxidation-deprotonation.

The formation of iminoxyl or phenoxyl radicals involves the (hardly exceptional) deprotonation of an O or N acid. However, in several cases, more complex

reaction sequences may be observed. We discuss two such cases, the formation of the anethole radical cation, **26**⁺, upon incorporation of *p*-propylanisole (**31**) and a deprotonation with ring opening observed upon incorporation of 1,2-diphenylcyclopropane. Incorporation of *p*-propylanisole (**31**) into the zeolite gives rise to an EPR spectrum that is incompatible with those observed for *p*-methylanisole and *p*-methylethoxybenzene radical cations (*vide supra*). Instead, it suggests that **31** is converted on the internal surfaces of the zeolite into the previously discussed anethole radical cation, **26**⁺. This conversion can be explained by three separate oxidation steps alternating with two deprotonations, a reaction sequence of unprecedented complexity for a room temperature reaction on the internal surfaces of the zeolite.⁵⁰ Alternatively, the initially formed radical cation may be dehydrogenated by an active site of the zeolite.



The final oxidation-deprotonation to be discussed is that of *trans*-1,2-diphenylcyclopropane (**32**). The radical cation of this substrate, **32**⁺, has been characterized by

a CIDNP study as a species with significant spin density on the two benzylic carbons and with sizeable hyperfine coupling constants for the benzylic as well as the geminal ^1H nuclei.¹² On the other hand, $32'^+$ has not as yet been characterized by an EPR spectrum. Since model considerations suggested that this substrate might fit into the cylindrical cavities (ID $\sim 5.5 \text{ \AA}$) of the zeolite, we attempted the generation of $32'^+$ on Na-ZSM-5. Surprisingly, the resulting EPR spectrum showed only one pair of ^1H nuclei with significant hyperfine coupling ($A = 11.5 \text{ G}$, 2 H; $A = 3.0 \text{ G}$, 6 H; Fig. 4).⁵⁹ Isotopic labeling of the geminal protons ($32\text{-}3\text{-}d_2$) produced an essentially identical EPR spectrum. This finding is compatible with two explanations; it may indicate that the geminal ^1H nuclei are at least two C–C bonds removed

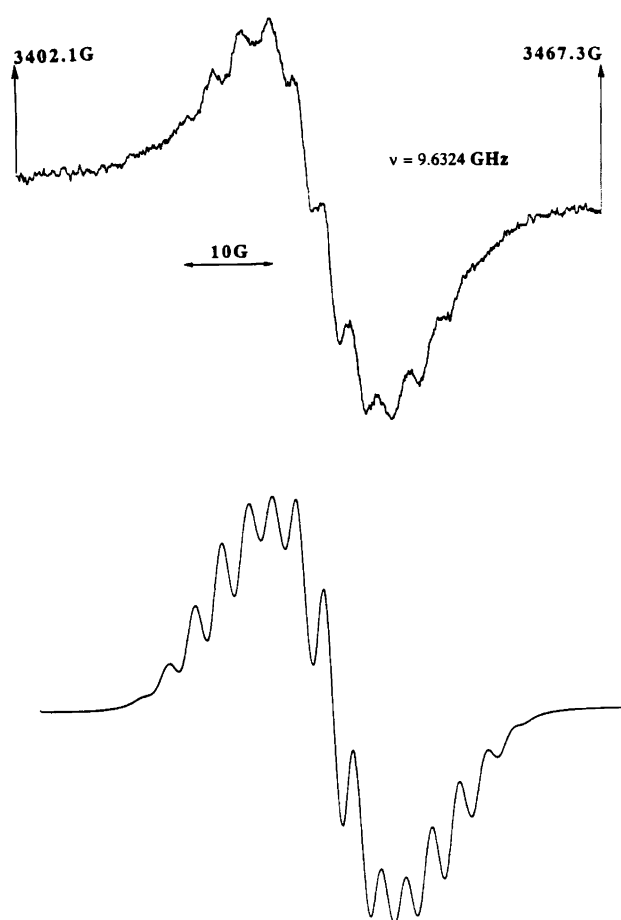
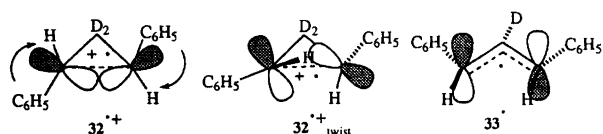


Fig. 4. (Top): X-Band EPR spectrum generated by incorporation of *trans*-1,2-diphenylcyclopropane (**32**) into the channels of pentasil zeolite (Na ZSM-5). The spectrum is identified as that of the *exo,exo*-1,3-diphenylallyl radical; (bottom) second-order⁶⁴ simulated spectrum,⁶⁵ an envelope of two Gaussian simulations, (1) a triplet of septets with $A_{2\text{H}} = 11.5 \text{ G}$ and $A_{6\text{H}} = 3.0 \text{ G}$, and a linewidth of 2.3 G, and (2) a broad line, with a linewidth of 17 G. The two spectra are simulated with relative intensities of 1:2.⁵⁹ The two components of the experimental spectrum have slightly different centers (g factors); the simulation program⁶⁵ only allows for the addition of isocentric spectra, resulting in a slight mismatch between simulation and experiment.

from the nearest center of spin density. Alternatively, the negligible hyperfine interaction of these nuclei may be due to their location in the nodal plane of the singly occupied molecular orbital (SOMO).

The key to the assignment lies in the known spectra of *endo,exo*- ($A_{\text{endo}} = 9.4 \text{ G}$; $A_{o,p} = 2.3 \text{ G}$; $A_{\text{exo}} = 14 \text{ G}$) and *exo,exo*-bisarylallyl radicals ($A_{\text{endo}} = 10.2 \text{ G}$; $A_{o,p} = 2.9 \text{ G}$).⁶⁰ Because the observed coupling constants are similar to the *endo*- ^1H nuclei of the allyl radical, we assign the spectrum to the *exo,exo*-1,3-diphenylallyl radical, $33'$, with two *endo*- ^1H nuclei. The formation of this species requires deprotonation of the initially formed radical cation ($32'^+$) with ring opening. The spectrum does not contain evidence for the timing of the two steps. We suggest a mechanism involving distortion of $32'^+$ in the direction towards the allyl radical. A distortion around the two benzylic cyclopropane centers will improve the poor overlap between the singly occupied cyclopropane Walsh orbital and the two secondary C–H (C–D) bonds. As a result, the deprotonation is assisted by overlap with the π -lobes. A conrotatory distortion not only provides a direct pathway to the *exo,exo*-substituted allyl radical, which is more readily accommodated in the zeolite channels, but also yields the correct symmetry for the singly occupied p-orbital.



To our knowledge, the interesting conversion of $32'^+$ into $33'$ is without precedent. Since the identification of $33'$ rests largely on the similarity of the hyperfine coupling constants of the diarylallyl radicals, a more rigorous confirmation of this assignment is currently in progress.

The examples of radical ion formation in Na-ZSM-5 zeolite and subsequent 'spontaneous' deprotonations show that in the channels of the zeolite deprotonation may be more prominent than in solution. The resulting radical cations are held rigidly in the channels of the zeolite, precluding the access of external reagents; this assignment readily accounts for their increased stability. The occasional complex reaction sequence, such as the conversion of **31** into $26'^+$ or of **32** into $33'$ are examples of zeolite-specific reactions. We are currently evaluating further zeolite-induced reactions.

Experimental

Materials and solvents. The donor/substrates, (1*R*,5*R*)-(+)- α -pinene (**6**) ($[\alpha]_{589} = +48$; 92% e.e.; Aldrich) and (1*S*,5*S*)-(–)- β -pinene (**9**) ($[\alpha]_{589} = -21$, 98% e.e.; Aldrich) were used as received. The electron acceptor/sensitizers, 1,4-dicyanobenzene (Aldrich; 98%), phenanthrene (Aldrich; 98%), 2,3,5,6-tetrachlorobenzoquinone (Aldrich, 98%) and biphenyl (Baker; 98%) were

purified by recrystallization. The solvents, acetonitrile (Fischer), methanol (Fischer), and dichloromethane (Fischer) were distilled from calcium hydride and stored over 4 Å molecular sieves in brown bottles under an argon atmosphere.

Photosensitized electron transfer reactions. The photoinduced electron transfer reactions were carried out with four different combinations of sensitizers/co-sensitizers and solvents. Reaction A was performed with 0.1 M donor and 0.05 M DCB in acetonitrile; reaction B used solutions of 0.1 M donor, 0.05 M DCB, and 0.02 M phenanthrene in acetonitrile-methanol (3 : 1); reaction C employed solutions containing 0.1 M donor, 0.05 M DCB, and 0.02 M biphenyl in acetonitrile-methanol (3 : 1 by volume); and reaction D was carried out with 0.1 M donor and 0.05 M 2,3,5,6-tetrachlorobenzoquinone (chloranil). Each solution was deoxygenated by being purged with argon for 15 min and irradiated in a Rayonet RPR-100 photoreactor equipped with sixteen RPR-3000 (runs A, C, and D) or RPR-3500 lamps (run B). The progress of the reactions was monitored by gas chromatography on a GC-MS system (HP 5890 series II GC interfaced with an HP 5971 mass selective detector), using a 12 m × 0.2 mm × 0.33 μm HP-1 capillary column (cross-linked methylsilicone on fused silica). Analytical runs were carried out in 4-mm ID NMR tubes stoppered with Latex stoppers, preparative runs in 30 mm ID tubes with central cooling fingers (water-cooling).

Isolation of products. Reaction products were isolated by column chromatographic procedures, carried out on columns of 2.5 or 1.2 cm ID, packed with 10–15 cm of silica gel (VWR Scientific, 230–400 mesh) and eluted with solvent gradients, usually from light petroleum (b.p. < 65 °C) to mixtures with ethyl acetate. Typically, several passes were required to isolate the products.

Characterization of products. Structure assignments of isolated products rest on MS and NMR data, including DEPT and two-dimensional COSY experiments, where needed. Extensive NOE difference spectra were taken to elucidate substituent stereochemistry and the spatial relationship between different groups, and to confirm the structure. Proton NMR spectra were recorded on either a Varian XL-400 or a Varian Gemini-200 spectrometer. ¹³C NMR spectra were recorded on a VXR or Gemini spectrometer, operating at 50.3 MHz.

Preparation of EPR samples. Na-ZSM-5 zeolite was thermally activated by calcination at 500 °C for 12 h and stored under argon. EPR samples were prepared by stirring 3–5 mg of the appropriate substrates with 70 mg of the zeolite in 10 ml of 2,2,4-trimethylpentane for 2 h. Upon mixing the reagents the zeolite showed light coloration, likely due to free radicals or radical ions on its external surface. The loaded zeolite was collected by filtration, washed with hexane, and dried under vacuum (0.001 Torr). Some of the coloration was removed by washing, suggesting that the corresponding radicals were

removed from the external surface of the zeolite. The dried zeolite samples were transferred to an EPR tube and their spectra recorded on a Bruker ESP 300 EPR spectrometer.

Results

Photoreactions of α-pinene. Reaction A. Irradiation of DCB-(1*R*,5*R*)-**6** ($[\alpha]_{589} = +48$; 92% e.e.)⁶¹ in acetonitrile without co-sensitizer or added methanol produced significant yields of a monocyclic isomer, limonene (~50%), and lesser yields of the acetonitrile adduct, **14** (21%) and an acyclic isomer, ocimene (5%). Three products, **11–13**, in which a *p*-cyanophenyl group has replaced a hydrogen atom were formed in significant yields (7–8% each; **11**: $[\alpha]_{546} = +170^\circ$; **12**: $[\alpha]_{546} = +100^\circ$; **13**: $[\alpha]_{546} = -141^\circ$).

Reaction B. When the reaction was carried out by irradiating DCB with phenanthrene as co-sensitizer in acetonitrile-methanol (3 : 1), the known photo NOCAS products, *cis*- and *trans*-**16**, and the acetonitrile adduct, **14**, were formed as major products. The yields of the isomeric hydrocarbons (<1%) and of the three substitution products (2–3%) were significantly reduced.

Reaction C. Irradiation of DCB with biphenyl as co-sensitizer in the presence of **6** in acetonitrile-methanol (3 : 1) gave rise mainly to the known photo NOCAS products, *cis*- (26%) and *trans*-**16** (28%), and the acetonitrile adduct **14** (14%). The monocyclic and acyclic isomers were obtained in yields of 15 and 2%, respectively; the 'substitution' products, **11–13**, were formed in minute yields (1–2%).

Reaction D. Irradiation of chloranil in the presence of (1*R*,5*R*)-**6** ($[\alpha]_{589} = +48$; 92% e.e.)⁶¹ in acetonitrile-methylene chloride gave rise to the monocyclic isomer, limonene, and a dehydrogenation product, verbenene, (1*R*,5*R*)-**8** ($[\alpha]_{589} = -86$; 92% e.e.; 8% yield).⁶² The photoreaction of chloranil and **6** was also studied in acetone and cyclohexane solutions. While the reaction of **6** proceeds smoothly in polar solvents (acetonitrile or acetone), its conversion is completely suppressed in non-polar media, such as cyclohexane.

Photoreactions of β-pinene. Reaction A. Irradiation of 1,4-dicyanobenzene and **9** in acetonitrile without co-sensitizer or added methanol produced mainly a monocyclic isomer, ψ-terpinene (55%). The acetonitrile adduct, **17** (15%), and an acyclic hydrocarbon (myrcene, 10%) were formed in lesser yields.

Reaction B. Irradiation of DCB-phenanthrene-(1*S*,5*S*)-**9** ($[\alpha]_{589} = -21$; 98% e.e.) in acetonitrile-methanol (3 : 1) gave rise mainly to the previously reported photo NOCAS products (**19** and two isomers, in ~55% combined yield), and to the acetonitrile adduct, **17** (~15%). In addition, the reaction produced minor yields of the three 4-cyanophenyl substituted products, **11–13** (e.g., **13**, $[\alpha]_{546} = -141$; 3%), and only trace amounts of the isomerization products (1%).

Reaction C. Irradiation of DCB with biphenyl as co-sensitizer in the presence of **9** in acetonitrile-methanol

(3:1) gave rise to the previously reported photo NOCAS products (**19** and two isomers, ~55% combined yield), and to the acetonitrile adduct **17** (~15%). The substitution products, **11–13** (1–2%), and the monocyclic and acyclic isomers (~1%) were formed in trace amounts.

Reaction D. Irradiation of chloranil in the presence of (1*S*,5*S*)-**9** ($[\alpha]_{589} = -21$; 98% e.e.)⁶³ in acetonitrile–methylene chloride yielded the endocyclic isomer, (1*S*,5*S*)-**6** ($[\alpha]_{589} = -48.7$; 94% e.e.)⁶¹ as the major product (~80%); the acetonitrile adduct, **17** (5%), was formed as a minor by-product. The photoreaction of chloranil and **9** was also studied in acetone and cyclohexane. The conversion of **9** proceeded smoothly in polar solvents (acetonitrile, acetone), but was completely suppressed in the non-polar medium, cyclohexane.

Structure assignments. Because of the importance of the correct structure assignments for the mechanistic conclusions, the spectral features revealing key elements of the products are discussed below. In addition to ¹H, ¹³C, and 2D COSY spectra, NOE difference spectra were recorded, where appropriate, to elucidate substituent stereochemistry and the spatial relationship between key ¹H nuclei.

Product **11** has one olefinic proton (H3, $\delta = 5.30$, qd, $J = 1.46, 2.86$ Hz), an allylic benzylic proton (H4, $\delta = 3.61$, dd, $J = 2.0$ Hz), and one bridgehead allylic signal (H1, $\delta = 1.12$, d, $J = 8.5$ Hz). The stereochemistry of the 4-(*p*-cyanophenyl) group rests on NOE evidence; pre-irradiation of the H4 frequency caused strong enhancement of one geminal methyl resonance (1.0 ppm). Accordingly, the 4-(*p*-cyanophenyl) group occupies the position *trans* to the geminal methyl groups.

Product **12** shows one olefinic proton (H3, $\delta = 5.26$, m), two allylic benzylic protons (H10, AB system, centered at $\delta = 3.32$, $J = 13.7$ Hz), one allylic bridgehead proton (H1, $\delta = 1.12$, d, $J = 8.6$ Hz), and two allylic protons (H4, $\delta = \sim 2.1$, m). A DEPT spectrum showed the presence of two CH carbons ($\delta = 46.0, 41.0$) and three CH₂ carbons ($\delta = 31.8, 32.3, 44.1$).

Product **13** ($[\alpha]_{546} = -141$) has two exocyclic methylene protons (4.50, 4.88), an allylic benzylic proton (H3, $\delta = 3.95$, dm, $J = 11.2$ Hz), and an allylic bridgehead proton (H1, $\delta = \sim 1.3$). The stereochemistry of the 3-(*p*-cyanophenyl) group was established by NOE experiments; pre-irradiation of the H3 resonance caused strong signal enhancement of one of the geminal methyl resonances (0.89 ppm). Therefore, the 3-(*p*-cyanophenyl) group occupies the position *trans* to the geminal methyl groups.

Verbenene **8** ($[\alpha]_{589} = -86$, molecular ion peak $M^{+ \cdot} = 134$) shows four olefinic protons, i.e., two exo-cyclo methylene protons ($\delta = 4.67$, d, $J = 2$ Hz; 4.69, d, $J = 2$ Hz) and two internal olefinic protons (H3, 6.05, d, $J = 8.6$ Hz; H4; 6.33, dd, $J = 6.12, 8.6$ Hz). Two bridgehead protons show signals at 1.50 ppm (H1, d, $J = 8.6$ Hz) and at 2.30 ppm (H5, q, $J = 6.12$ Hz). The identification of product **8** as verbenene was confirmed by the ¹H 2D

COSY spectrum. One bridgehead proton, H1 was coupled only to one bridge proton (H7, $\delta = 2.55$, ddd, $J = 8.6, 5.5, 5.5$ Hz), whereas the other, H5, showed cross-peaks with three protons (H4; H7_{syn}, $\delta = 2.55$, ddd, $J = 8.6, 5.5, 5.5$ Hz; H7_{anti}, $\delta = 2.65$, dd, $J = 6.12, 5.6, 1.6$ Hz).

Acknowledgements. Financial support of this work by the National Science Foundation through grants NSF CHE-9110487 and CHE-9414271 and an equipment grant NSF CHE-9107839 is gratefully acknowledged.

References

- Yoshida, K. *Electrooxidation in Organic Chemistry: the Role of Cation Radicals as Synthetic Intermediates*, Wiley, New York 1984.
- Shida, T. *Electronic Absorption Spectra of Radical Ions*, Elsevier, Amsterdam 1988.
- Lund, A. and Shiotani, M., Eds., *Radical Ionic Systems*, Kluwer, Dordrecht 1991.
- Shida, T., Haselbach, E. and Bally, T. *Acc. Chem. Res.* **17** (1984) 180.
- Roth, H. D. *Acc. Chem. Res.* **20** (1987) 343.
- Haddon, R. C. and Roth, H. D. *Croat. Chem. Acta* **57** (1984) 1165.
- Roth, H. D. *Top. Curr. Chem.* **163** (1992) 133.
- Farid, S., Hartman, S. E. and Evans, T. R. In: Gordon, M. and Ware, W. R., Eds., *The Exciplex*, Academic Press, New York 1975, pp. 327–343.
- Neunteufel, R. A. and Arnold, D. R. *J. Am. Chem. Soc.* **95** (1973) 4080.
- Pac, C., Nakasone, A. and Sakurai, H. *J. Am. Chem. Soc.* **99** (1977) 5808.
- Arnold, D. R. and Maroulis, A. J. *J. Am. Chem. Soc.* **99** (1977) 7355.
- Roth, H. D. and Schilling, M. L. M. *J. Am. Chem. Soc.* **101** (1979) 1898.
- Roth, H. D., Schilling, M. L. M. and Jones, G., II. *J. Am. Chem. Soc.* **103** (1981) 1246.
- Dinnocenzo, J. P. and Schmittel, M. *J. Am. Chem. Soc.* **109** (1987) 1561.
- Schmittel, M. and von Seggern, H. *J. Am. Chem. Soc.* **115** (1993) 2165.
- Weng, H., Sheik, Q. and Roth, H. D. *J. Am. Chem. Soc.* **117** (1995) 10656.
- Mattes, S. L. and Farid, S. In: Padwa, A., Ed., *Organic Photochemistry*, Marcel Dekker, New York 1983, Vol. 6, pp. 233–326.
- Gould, I. R., Young, R. H., Mueller, L. J. and Farid, S. *J. Am. Chem. Soc.* **116** (1994) 8176.
- Lakkaraju, P. S., Zhang, J. and Roth, H. D. *J. Chem. Soc., Chem. Commun.* (1994) 1969.
- Ramamurthy, V., Casper, C. V. and Corbin, D. R. *J. Am. Chem. Soc.* **113** (1991) 594.
- Ramamurthy, V., Casper, C. V. and Corbin, D. R. *J. Am. Chem. Soc.* **113** (1991) 600.
- Lakkaraju, P. S., Zhang, J. and Roth, H. D. *J. Chem. Soc., Perkin Trans. 2* (1993) 2319.
- Lakkaraju, P. S., Zhang, J. and Roth, H. D. *J. Phys. Chem.* **98** (1994) 2722.
- Arnac, M. and Verboom, G. *Anal. Chem.* **49** (1977) 806.
- Sullivan, A. B. and Reynolds, G. F. *J. Phys. Chem.* **80** (1976) 2671.
- Krynkov, A. I., Platonova, E. P. and Krasnova, V. A. *Zh. Obshch. Khim.* **48** (1978) 2583.
- Handoo, K. L. and Gadru, K. *Curr. Sci.* **55** (1986) 920.

28. Stallings, M. D., Morrison, M. M. and Sawyer, D. T. *Inorg. Chem.* 20 (1981) 2655.
29. Zhou, D., Sheik M. and Roth, H. D. *Tetrahedron Lett.* 37 (1996) 2385.
30. Arnold, D. R. and Du, X. *J. Am. Chem. Soc.* 111 (1989) 7666.
31. Arnold, D. R. and Du, X. *Can. J. Chem.* 72 (1994) 403.
32. Rao, V. R. and Hixson, S. S. *J. Am. Chem. Soc.* 101 (1979) 6458.
33. Arnold, D. R. and Snow, M. S. *Can. J. Chem.* 66 (1988) 3012.
34. Reynolds, D. W., Hairirchian, B., Chiou, H.-S., Marsh, B. K. and Bauld, N. L. *J. Phys. Org. Chem.* 2 (1989) 57.
35. Bauld, N. L. *J. Comput. Chem.* 11 (1990) 896.
36. Weng, H., Scarlata, C. and Roth, H. D. *J. Am. Chem. Soc.* 118 (1996) 10947.
37. Derouane, E. G., Lemos, F., Naccache, C. and Rebeiro, F. R., Eds., *Zeolite Microporous Solids: Synthesis, Structure, and Reactivity*, Kluwer, Dordrecht 1991.
38. Stucky, G. D. and Dwyer, F. D., Eds., *Intrazeolite Chemistry*, ACS Monograph 1983, Vol. 218.
39. Rabo, J. A., Ed., *Zeolite Chemistry and Catalysis*, ACS Monograph 1976, Vol. 171.
40. Rhodes, C. J. and Hinds, C. S. In: Lund, A. and Rhodes, C. J., Eds., *Radicals on Surfaces*, Kluwer, Dordrecht 1995, pp. 119–145.
41. Chen, F. and Guo, X. *J. Chem. Soc., Chem. Commun.* (1989) 1682.
42. Kasai, P. H., Bishop, R. J. In: Rabo, J. A., Ed., *Zeolite Chemistry and Catalysis*, American Chemical Society, Washington, DC 1976, p. 350.
43. Cano, M. L., Gorma, A., Fornes, V. and Garcia, H. *J. Phys. Chem.* 99 (1995) 4241.
44. Li, X., Iu, K. K., Thomas, J. K., He, H. and Klinowski, J. *J. Am. Chem. Soc.* 116 (1994) 11811.
45. Chen, F. R. and Fripiat, J. J. *J. Phys. Chem.* 96 (1992) 819.
46. Dixon, W. T. and Murphy, D. *J. Chem. Soc., Perkin Trans. 2* (1976) 1823.
47. Ebersson, L., Hartshorn, M. P. and Persson, O. *J. Chem. Soc., Perkin Trans. 2* (1995) 1735.
48. Elson, I. H. and Kochi, J. K. *J. Am. Chem. Soc.* 95 (1973) 5060.
49. Hewgill, F. R., Legge, F. and Webb, R. *Aust. J. Chem.* 46 (1993) 1605.
50. Lakkaraju, P. S., Zhou, D. and Roth, H. D. *J. Chem. Soc., Chem. Commun.* In press.
51. Roth, H. D. In Muus, L. T., Atkins, P. W., McLauchlan, K. A. and Pedersen, J. B., Eds., *Chemically Induced Magnetic Polarization: Theory, Technique, and Applications*, NATO Adv. Study Inst. Ser. C, Vol. 34; Reidel, Dordrecht, Holland 1977; p. 39.
52. Eckert, G. and Goetz, M. *J. Am. Chem. Soc.* 116 (1994) 11999.
53. Goetz, M. and Eckert, G. *J. Am. Chem. Soc.* 118 (1996) 140.
54. Brede, O., David, F. and Steenzen, S. *J. Chem. Soc., Perkin Trans. 2* (1995) 23.
55. Stone, T. J. and Waters, W. A. *Proc. Chem. Soc.* (1962) 253.
56. Stone, T. J. and Waters, W. A. *J. Chem. Soc.* (1964) 213.
57. Dixon, W. T., Moghimi, M. and Murphy, D. *J. Chem. Soc. Faraday Trans. 2* (1974) 1713.
58. Jackson, R. A. and Hosseini, K. M. *J. Chem. Soc., Chem. Commun.* (1992) 967.
59. Herbertz, T., Roth, H. D. and Lakkaraju, P. S. *J. Am. Chem. Soc. Submitted.*
60. Berndt, A. In: Forrester, R. A., Ishizu, K., Kothe, G., Nelsen, S. F., Ohya-Nishiguchi, H., Watanabe, K. and Wilker, K. 'Organic Cation Radicals and Polyradicals' in *Landolt Börnstein, Numerical Data and Functional Relationships in Science and Technology*, Volume IX, Part d2, Springer Verlag, Heidelberg 1980, pp. 391, 392.
61. Comyns, A. E. and Lucas, H. *J. Am. Chem. Soc.* 79 (1957) 4339.
62. Moore, R. N. and Fisher, G. S. *J. Am. Chem. Soc.* 78 (1956) 1173.
63. Fugitt, R. E., Stallcup, W. D. and Hawkins, J. E. *J. Am. Chem. Soc.* 64 (1942) 2978.
64. Fessenden, R. W. *J. Chem. Phys.* 37 (1962) 747.
65. Heikki, J. *Comput. Chem.* 12 (1988) 189.

Received July 17, 1996.